Ultrafast Photoinduced Electron Transfer in a Chlorophyll-Based Triad: Vibrationally Hot Ion Pair Intermediates and Dynamic Solvent Effects

Gary P. Wiederrecht,† Mark P. Niemczyk,† Walter A. Svec,† and Michael R. Wasielewski*,†,‡

Contribution from the Chemistry Division, Argonne National Laboratory, Argonne, Illinois 60439, and Department of Chemistry, Northwestern University, Evanston, Illinois 60208

Received September 14, 1995[⊗]

Abstract: We report ultrafast transient absorption studies of photoinduced electron transfer in the triad molecule zinc methyl 13[1]-desoxopyropheophorbide *a*−pyromellitimide−1,8:4,5-naphthalenediimide (ZC−PI−NI) in solution. The absorption spectra of the radical anions of PI and NI possess narrow and well-separated absorption bands which permit the direct observation of both the intermediate and final charge-separated states. Selective optical excitation of the ZC donor results in the formation of the intermediate charge-separated state, ZC^+-PI^--NI, in less than 2 ps in nonpolar solvents. The PI radical ion within the ZC^+-PI^--NI intermediate is vibrationally excited as illustrated by time-dependent changes in the band shape of its transient absorption spectrum. The rate of the initial charge separation reaction forming ZC^+-PI^--NI and the subsequent charge shift reaction to form the final state, $ZC^+-PI-NI^-$, as well as the appearance of the vibrationally excited intermediate are all highly solvent dependent even for solvents with similar dielectric constants. Analogous dyad control molecules ZCPI and ZCNI were also studied and compared with the results for ZCPINI.

Introduction

The initial photoinduced electron transfer events in the reaction center proteins from purple photosynthetic bacteria and green plants occur on a time scale of a few picoseconds.[1,2] Several recent attempts to model this photochemical electron transfer process have employed chlorophyll- or porphyrin-based electron donor−acceptor molecules that undergo photoinduced charge separation on a similar time scale. The electron donors and acceptors in these model systems are separated by rigid spacer groups or by hydrogen bonding networks that maintain restricted distances and orientations between the donors and acceptors.[3−16] Studies of the radical ion pair intermediates that result from photochemical charge separation in these models provide clues to the mechanism of long-distance electron transfer.

Both natural and artificial photosynthetic systems that undergo sufficiently rapid charge separation may produce vibrationally hot radical ion pair intermediates. In principal, the observation of such intermediates in a particulr photosynthetic model system can reveal the course of excess energy redistribution within the donor−acceptor assembly and transfer of this energy to the medium surrounding the assembly. Doorn et al. were the first to observe condensed phase vibrational excitation coupled to electron transfer in the transition metal complex $[(NC)_5M^{II}-CNM^{III}(NH_3)_5]^-$ (M = Ru,Os), which forms the redox isomer $[(NC)_5M^{III}CNM^{II}(NH_3)_5]^-$ upon optical excitation of its charge transfer band.[17] Spears et al. have observed vibrational relaxation by optically exciting the charge transfer band of $[Co(Cp)_2^+|Co(CO)_4^-]$ and by observing the CO stretching modes of the vibrationally hot fragment $Co(CO)_4$ using picosecond infrared absorption spectroscopy.[18] Studies of vibrational relaxation in the ground and excited states of larger organic molecules have shown that intramolecular relaxation within the vibrationally excited ground state generally occurs in a few picoseconds or less, and energy transfer to the solvent occurs in roughly 10 ps.[19−21] Wynne et al. recently observed a 570 fs relaxation that may be due to vibrational relaxation in

† Argonne National Laboratory.
‡ Northwestern University.
[⊗] Abstract published in *Advance ACS Abstracts,* December 15, 1995.

(1) Finkele, U.; Lauterwasser, C.; Struck, A.; Scheer, H.; Zinth, W. *Proc. Natl. Acad. Sci. U.S.A.* **1992**, *89*, 9514.
(2) Wiederrecht, G. P.; Seibert, M.; Govindjee, Wasielewski, M. R. *Proc. Natl. Acad. Sci. U.S.A.* **1994**, *91*, 8999.
(3) Wasielewski, M. R. *Chem. Rev.* **1992**, *92*, 435.
(4) Gust, D.; Moore, T. A.; Moore, A. L. *Acc. Chem. Res.* **1993**, *26*, 198.
(5) Kurreck, H.; Huber, M. *Angew. Chem., Int. Ed. Engl.* **1995**, *34*, 849.
(6) Gust, D.; Moore, T. A.; Moore, A. L.; Lee, S.-J.; Bittersmann, E.; Luttrull, D. K.; Rehms, A. A.; DeGraziano, J. M.; Ma, X. C.; Gao, F.; Belford, R. E.; Trier, T. T. *Science* **1990**, *242*, 199.
(7) Rodriguez, J.; Kirmaier, C.; Johnson, M. R.; Friesner, R. A.; Holten, D.; Sessler, J. L. *J. Am. Chem. Soc.* **1991**, *113*, 1652.
(8) Sakata, Y.; Tsue, H.; O'Neil, M. P.; Wiederrecht, G. P.; Wasielewski, M. R. *J. Am. Chem. Soc.* **1994**, *116*, 6904.
(9) Johnson, D. G.; Niemczyk, M. P.; Minsek, D. W.; Wiederrecht, G. P.; Svec, W. A.; G. L. Gaines, I.; Wasielewski, M. R. *J. Am. Chem. Soc.* **1993**, *115*, 5692.
(10) Wiederrecht, G. P.; Watanabe, S.; Wasielewski, M. R. *Chem. Phys.* **1993**, *176*, 601.
(11) Lawson, J. M.; Paddon-Row, M. N.; Schuddeboom, W.; Warman, J. M.; Clayton, A. H. A.; Ghiggino, K. P. *J. Phys. Chem.* **1993**, *97*, 13099.
(12) Sessler, J. L.; Capuano, V. L.; Harriman, A. *J. Am. Chem. Soc.* **1993**, *115*, 4618.
(13) Sessler, J. L.; Wang, B.; Harriman, A. *J. Am. Chem. Soc.* **1995**, *117*, 704.
(14) Turro, C.; Chang, C. K.; Leroi, G. E.; Cukier, R. I.; Nocera, D. G. *J. Am. Chem. Soc.* **1992**, *114*, 4103.
(15) Roberts, J. A.; Kirby, J. P.; Nocera, D. G. *J. Am. Chem. Soc.* **1995**, *117*, 8051.
(16) Wynne, K.; LeCours, S. M.; Galli, C.; Therien, M. J.; Hochstrasser, R. M. *J. Am. Chem. Soc.* **1995**, *117*, 3749.
(17) Doorn, S. K.; Dyer, R. B.; Stoutland, P. O.; Woodruff, W. H. *J. Am. Chem. Soc.* **1993**, *115*, 6398.
(18) Spears, K. G.; Wen, X.; Arrivo, S. M. *J. Phys. Chem.* **1994**, *98*, 9693.
(19) Seilmeier, A.; Scherer, P. O. J.; Kaiser, W. *Chem. Phys. Lett.* **1984**, *105*, 140.
(20) Wondrazek, F.; Seilmeier, A.; Kaiser, W. *Chem. Phys. Lett.* **1984**, *104*, 121.
(21) Gottfried, N. H.; Seilmeier, A.; Kaiser, W. *Chem. Phys. Lett.* **1984**, *111*, 326.

0002-7863/96/1518-0081$12.00/0

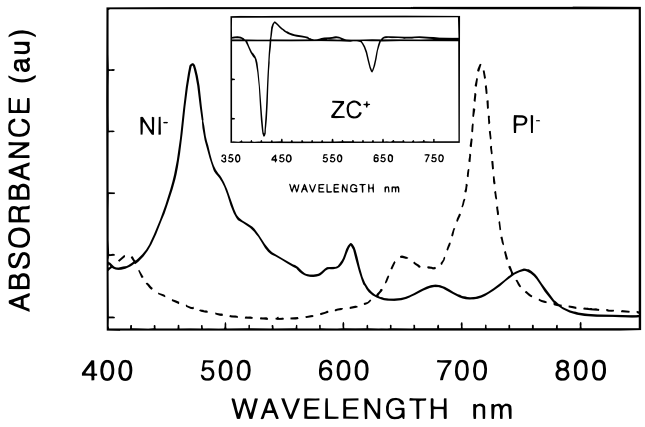

Figure 1. Spectra of PI^- and NI^- in DMF are shown. The well-separated peaks in the absorption spectra permit easy observation of the intermediate and final charge-separated states of ZCPINI. The inset shows the difference spectrum of $ZC^+ - ZC$. Note that the ground state PI and NI chromophores do not have any significant absorption in the spectral region shown.

a covalently-linked porphyrin−quinone molecule in which the donor and acceptor are strongly coupled electronically.[16] Thus, photosynthetic model systems may undergo charge separation on a time scale comparable to that of vibrational relaxation.

Observation of vibrationally excited intermediates in photosynthetic model systems is difficult because the biologically relevant chromophores usually have overlapping and featureless excited state and radical ion spectra, which render observation of spectral broadening due to vibrational excitation nearly impossible. However, progress has been made toward developing donors and acceptors that possess more distinct spectral signatures.[22−25] For example, Osuka et al. have recently employed pyromellitimides as acceptors in multicomponent artificial photosynthetic systems.[23] The pyromellitimide moiety (PI) is easily reduced at approximately −0.8 V vs SCE and possesses a distinctive intense and narrow absorption at 720 nm ($\epsilon \approx 4 \times 10^4$ M^{-1} cm^{-1}) as shown in Figure 1. These properties, combined with its synthetic accessibility, make the pyromellitimide acceptor very useful for electron transfer studies. Ohkohchi et al. recently prepared a zinc porphyrin−PI−quinone triad and were able to observe the intermediate radical ion pair.[25] However, since the quinone radical anion possesses weak spectral features that are overwhelmed by those of the porphyrin cation, no direct spectral evidence of the reduction of the quinone was observed. Thus, these systems are difficult to fully characterize because they lack a full complement of relevant spectral features.

To overcome these difficulties we have designed the novel triad system zinc methyl 13[1]-desoxopyropheophorbide *a*−pyromellitimide−1,8:4,5-naphthalenediimide (ZCPINI). Selective photoexcitation of ZC results in the formation of an intermediate charge-separated state, ZC^+PI^-NI. This is followed by a charge shift to form ZC^+PINI^-. As illustrated in Figure 1, the strongest spectral feature of NI^- occurs at 470 nm ($\epsilon \approx 3 \times 10^4$ M^{-1} cm^{-1}) and is well separated from the PI^- absorption band. This permits the unambiguous observation of both the intermediate and final charge-separated states on the electron transfer pathway

(22) Mataga, N.; Kanda, Y.; Asahi, T.; Miyasaka, H.; Okada, T. *Chem. Phys.* **1988**, *127*, 239.
(23) Osuka, A.; Nakajima, S.; Maruyama, K.; Mataga, N.; Asahi, T.; Yamazaki, I.; Nishimura, Y.; Ohno, T.; Nozaki, K. *J. Am. Chem. Soc.* **1993**, *115*, 4577.
(24) Asahi, T.; Ohkohchi, M.; Matsusaka, R.; Mataga, N.; Zhang, R. P.; Osuka, A.; Maruyama, K. *J. Am. Chem. Soc.* **1993**, *115*, 5665.
(25) Ohkohchi, M.; Takahashi, A.; Mataga, N.; Okada, T.; Osuka, A.; Yamada, H.; Maruyama, K. *J. Am. Chem. Soc.* **1993**, *115*, 12137.

Table 1. Electrochemical Data and Free Energies of Reaction for ZCPI, ZCNI, and ZCPINI in Benzonitrile

ion pair[a]	redn potent of acceptor (eV)	r_{12} (Å)	ΔG_{CS} (eV)	ΔG_{CR} (eV)
ZC^+PI^-	−0.87	11	−0.68	−1.27
ZC^+NI^-	−0.60	11	−0.95	−1.00
ZC^+PI^-NI	−0.76	11	−0.79	−1.16
ZC^+PINI^-	−0.41	18	−1.16[b]	−0.79

[a] The oxidation potential of ZC is 0.43 V vs SCE, and the energy of its lowest excited singlet state is 1.95 eV. [b] ΔG_{CS} for the reaction $ZC^*PINI \rightarrow ZC^+PINI^-$.

of ZCPINI by time-resolved transient absorbance measurements. In order to obtain fast photoinitiated charge separation rates that are comparable to typical rates of vibrational relaxation in condensed media, ZCPINI employs a 13[1]-desoxopyropheophorbide *a* donor that oxidizes at 0.43 V vs SCE, which is approximately 0.2 V less positive than the oxidation potential of more frequently used porphyrins and chlorins. Using the easily reduced PI and NI acceptors, charge separation time constants of 130 fs to 1.8 ps are observed in low-polarity solvents, such as toluene, benzene, *p*-dioxane, and *o*-xylene. The corresponding dyad molecules, ZCPI and ZCNI, are used as control molecules to better understand the processes occurring in the ZCPINI triad. The very fast charge separation to form the ZC^+PI^-NI intermediate allows us to observe this ion pair intermediate in a vibrationally hot state. This is largely due to favorable rate constants for charge separation in some of the solvents, which allow ZC^+PI^-NI to form faster than the vibrational relaxation time of PI^-, while at the same time allowing the lifetime of ZC^+PI^-NI to be long enough to actually observe vibrational relaxation.

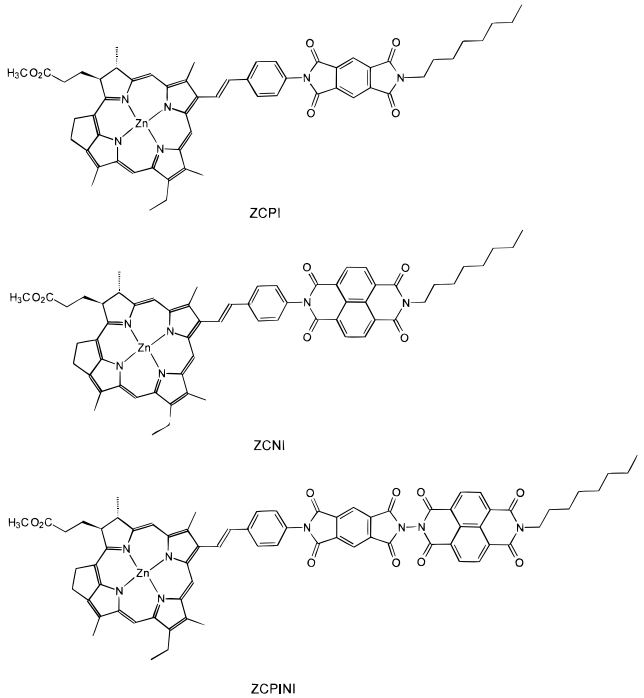

Results

Electrochemical Data. The charge transfer rates in the triad are considerably larger than those observed in the dyad control molecules. The redox potentials given in Table 1 begin to explain this observation. Table 1 shows that the PI and NI acceptors are more easily reduced by 0.1−0.2 V when they exist as a coupled species. This is presumably due to the mutual

substituent effect of electron-withdrawing diimides on each other, leading to a larger driving force for electron transfer and, thus, faster charge separation within the triad as compared to the dyads. Table 1 illustrates the approximate free energy of charge separation (ΔG_{CS}) and charge recombination (ΔG_{CR}) for ZCPI, ZCNI, and ZCPINI in benzonitrile. For polar solvents, these values are given by the following relations:

$$\Delta G_{CS} = E_{OX} - E_{RED} - \frac{{e_0}^2}{\epsilon_s r_{12}} - E_S \quad (1)$$

$$\Delta G_{CR} = -\Delta G_{CS} - E_S \quad (2)$$

where E_{OX} is the oxidation potential of ZC, E_{RED} is the reduction potential for the selected acceptor, E_S is the energy of the first excited singlet state of the ZC donor (1.95 eV), e_o is the charge of an electron, ϵ_s is the static dielectric constant of the solvent (ranging from 2.2 to 2.5 for the solvents utilized), and r_{12} is the spacing between the donor and acceptor. For the low-polarity solvents employed here, the solvation energies of the ions must also be considered. The solvation energies of the ions pairs in low-polarity solvents are difficult to calculate accurately, but calculations based on dielectric continuum theory[26] and experimental estimates[27] suggest that the energy levels of the initially formed ion pairs at a distance of 11 Å are approximately 0.6 eV higher than those determined from eqs 1 and 2. Therefore, in these low-polarity solvents, $\Delta G_{CS} \cong -0.2$ eV for the reaction ZC*PINI $\rightarrow$ ZC^+PI^-NI. For the subsequent charge shift reaction $ZC^+PI^-NI \rightarrow ZC^+PINI^-$ in the same low-polarity solvents, both ion pairs are solvated so that the differences in E_{RED} for formation of PI^- and NI^- and in Coulomb energies of the ZC^+PI^-NI and ZC^+PINI^- ion pairs can be used to calculate $\Delta G_{CS} \cong -0.13$ eV.

Coupling two redox centers together within a single structure is well-known to often result in changes in the redox potentials of the individual centers. The effects of these changes on rates of electron transfer within artificial photosynthetic systems have been discussed only sparingly in the electron transfer literature. In one recent example Osuka et al. have shown that the oxidation potential of a donor that consists of two zinc porphyrins covalently attached by a 1,2-phenylene bridge is 0.23 V less positive than the corresponding potential of a single zinc porphyrin.[23] They also found that the diporphyrin possesses an S_1 state energy that is 0.24 eV lower than that of the porphyrin. Of course, the driving force for electron transfer does not change if both E_s and the oxidation potential of the donor both decrease. As described in more detail below, the changes in the reduction potentials of PI and NI that occur when these acceptors are covalently linked within ZCPINI makes ΔG_{CS} more negative with the desirable result that charge separation occurs faster within ZCPINI than within the corresponding dyads.

Transient Absorption Data. Figure 2 shows the ground state absorption spectrum of the ZC donor chromophore. Excitation of ZC at 640 nm occurs on the red edge of the $Q_y(0,0)$ band which was chosen in order to minimize possible contributions to electron transfer rates from processes associated with its vibrationally excited S_1 state or higher electronic states.

Figure 3 shows the transient absorption kinetics at 470 nm for ZCNI and ZCPINI in *p*-dioxane, while the inset shows the long time decay of the transient absorption at 720 nm. The large difference in both the forward and back electron transfer rates for the triad versus the dyad is illustrated. The triad data is characterized by a fast decay of 1.9 ps, followed by a 2.2 ns decay and a long-lived shelf. We attribute the initial decay at 470 nm to the decay of ZC* to ZC^+. The 2.2 ns is assigned to the decay of the final charge-separated state, ZC^+PINI^-. The long-lived shelf is assigned to a small amount of ^3ZC formed possibly as a result of the radical ion pair recombination reaction. These results can be compared to the electron transfer process within the ZCPI dyad, which has a formation time of 15 ps and a lifetime of approximately 41 ps. Electron transfer occurs nearly 1 order of magnitude faster within the triad, and the charge-separated state lives roughly 50 times longer than that of the analogous dyad. This compares to a factor of 40 for the best case zinc porphyrin−PI−quinone triad work of Ohkohchi et al.[25] Table 2 shows the formation times and lifetimes of the intermediate and final charge-separated states in toluene and *p*-dioxane.

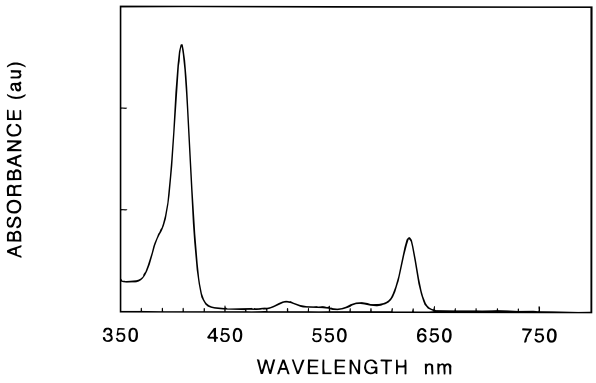

Figure 2. Ground state absorption spectrum of ZC in *p*-dioxane is shown.

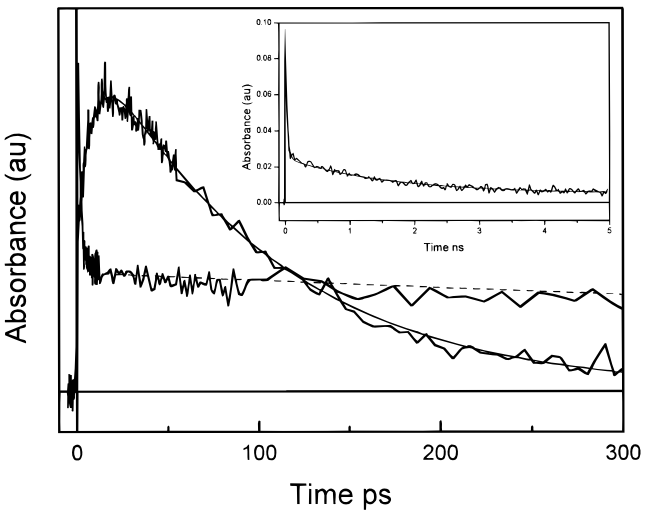

Figure 3. Absorption kinetics at 470 nm of ZCNI and ZCPINI in *p*-dioxane are shown. The data illustrate the faster charge separation and longer lived ion pair state in the triad vs the dyad. The inset is a long time scan with a probe wavelength at 720 nm, which has superior signal to noise compared to the 470 nm data.

Figure 4 illustrates the transient absorption spectra of the triad. Clear bands at 720 and 470 nm show the appearance of the intermediate and final charge transfer states. The spectra of the PI^- absorption band at 720 nm are very intriguing. Upon the initial appearance of PI^-, the band has an enhanced tail on the red edge out to approximately 800 nm. This spectral feature may indicate the formation of a vibrationally excited PI^- band. Before drawing any conclusions about the PI^- band, it is important to first determine the contributions of the ZC excited state and cation to the absorption signal in this part of the spectrum. We therefore obtained similar spectra for ZCNI that

(26) Weller, A. *Z. Phys. Chem. (Munich)* **1982**, *133*, 93.
(27) Wasielewski, M. R.; Gaines, G. L., III; O'Neil, M. P.; Svec, W. A.; Niemczyk, M. P.; Prodi, L.; Gosztola, D. In *Dynamics and Mechanics of Photoinduced Transfer and Related Phenomena*; Mataga, N., Okada, T., Masuhara, H., Eds.; Elsevier: New York, 1992; pp 87.

Table 2. Electron Transfer 1/*e* Times for ZCPI, ZCNI, and ZCPINI in *p*-Dioxane and Toluene

		p-dioxane		toluene	
molecule	chromophore	τ_{CT}	τ_{CR}	τ_{CT}	τ_{CR}
ZCPI	PI^-	21	48	25	83
ZCPI	ZC*	15	41	*a*	81
ZCNI	NI^-	8.6	100	13	330
ZCNI	ZC*	2.9	90	3.7	360
ZCPINI	PI^-	1.6	44	<0.13	1.7
ZCPINI	NI^-	59	2200	1.7	140
ZCPINI	ZC*	1.9	2200	<0.13	140

[a] This value was not able to be determined due to small differences in the absorption cross section of the excited state and cationic states of ZC in toluene.

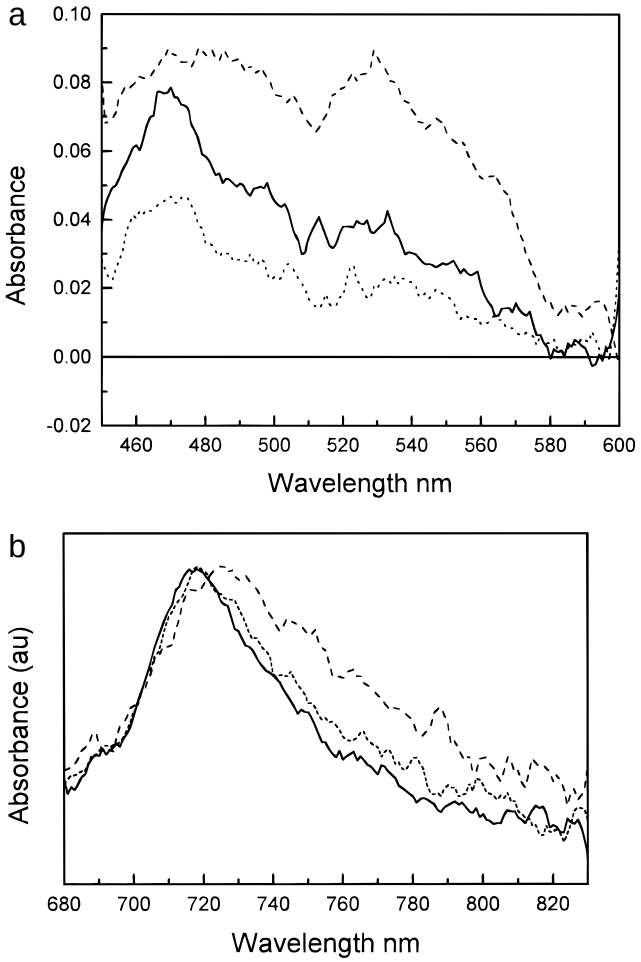

Figure 4. (a) Transient spectra of ZCPINI in *p*-dioxane in the blue region for time delays of (- - -) 3 ps, (—) 90 ps, and (•••) 1 ns. The data illustrate the appearance of the NI^- absorption band at 475 nm. (b) Transient spectra of ZCPINI in the red region for time delays of (- - -) 1.6 ps, (•••) 6.6 ps, and (—) 11.6 ps. Vibrational excitation of PI^- is suggested by the red-enhanced tail of the 720 nm band.

are illustrated in Figure 5. In this region, only a relatively weak NI^- absorption band centered at 760 nm contaminates the spectrum, with the remainder of the signal due to the excited and cationic states of ZC. The spectrum at the earliest time delay shows that the excited state of ZC is dominated by a flat absorption to the red of 720 nm and a stimulated emission feature at 700 nm. The emission is not specific to ZCNI as it is also present at early times in ZCPI data, and the decay kinetics of this feature match the decay of ZC* to ZC^+ in both cases. Upon formation of the ZC^+NI^- ion pair, a weak absorption of ZC^+ at 720 nm is observed. However, the data in Figure 5 further indicate that the excited state to cationic state spectral

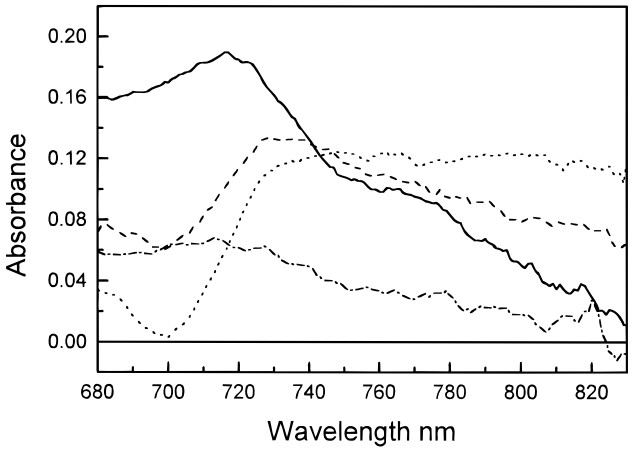

Figure 5. Transient spectra of ZCNI in *p*-dioxane for the 680−830 nm spectral region for time delays of (•••) 800 fs, (- - -) 2.8 ps, (—) 26 ps, and (— - —) 136 ps. The fully formed cation spectrum is represented for the time delay of 26 ps, with only a slight contribution from the 760 nm band of NI^-.

changes are not contributing to the signal of Figure 4b because the emission band is not observed at these times. In other words, the cation has already formed 1.6 ps after optical excitation.

In order to further interpret the cause of the spectral broadening shown in Figure 4, the transient absorption kinetics at 720 nm for ZCPINI in *p*-dioxane and toluene are illustrated in Figure 6. The data for *p*-dioxane show an initial decay of 1.6 ps, in good agreement with the formation time of ZC^+ determined at 810 nm. This decay is followed by a 4.5 ± 0.5 ps rise, which correlates with the narrowing of the 720 nm band. This time scale suggests that intermolecular energy transfer to the solvent, and not intramolecular energy redistribution, is principally responsible for the vibrational relaxation of PI^-. In order to further verify this conclusion, temperature-dependent studies of the kinetics of this feature were also performed. Data were obtained to 286 K, because the freezing point of *p*-dioxane is 285 K. The 1/*e* time for vibrational relaxation at the lowest temperature was 8.6 ps, as opposed to 4.5 ps at room temperature. This is qualitatively consist with vibrational relaxation of the intermediate through translational collisions of the solvent with ZCPINI. As the solvent becomes more viscous, the translational energy of the solvent decreases. If this effect is primarily intramolecular in nature, such a small temperature change would not be expected to significantly affect the relaxation time.

Figure 6 also gives a dramatic indication of the effect of the solvent on charge transfer rates in ZCPINI, even for solvents with similar dielectric constants. In contrast to the *p*-dioxane data, a single exponential decay of 1.7 ps is observed in toluene, followed by the long-lived charge-separated state. Furthermore, the spectra illustrated in Figure 7 show that a state with charge transfer character is formed on a pulse width limited time scale in toluene because the data taken immediately following excitation do not have any of the excited state features shown in Figure 5. The spectrum at 300 fs is sharper at 720 nm than the cation spectrum shown in Figure 5, indicating that there is already a contribution from the PI^- band. The spectra taken after the fast decay indicate only the presence of ZC^+ and NI^-. Therefore, we believe that ZC^+PI^-NI is formed on a pulse width limited time scale (<130 fs) in toluene and that it subsequently charge separates further to ZC^+PINI^- in 1.7 ps. Also, the ZC^+PINI^- ion pair has a lifetime of only 200 ps in toluene vs 2 ns in *p*-dioxane. Additional solvents were used: benzene appears to be similar to toluene, whereas *o*-xylene is similar to *p*-dioxane. It is evident that solvent characteristics other than

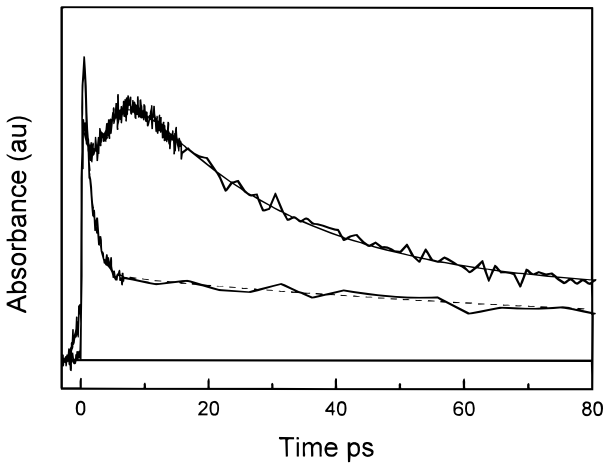

Figure 6. Transient absorption kinetics for ZCPINI at 720 nm in *p*-dioxane (solid fit) and toluene (dashed fit). The *p*-dioxane data possess a fast decay of 1.6 ps, followed by a rise of 4.5 ps. This component is due to the vibrational relaxation of the PI^- chromophore. The 26 ps decay is due to charge recombination to form ZCPINI and charge shift to form ZC^+PINI^-. The toluene data consist of a fast decay of 1.7 ps to the final ZC^+PINI^- charge-separated state.

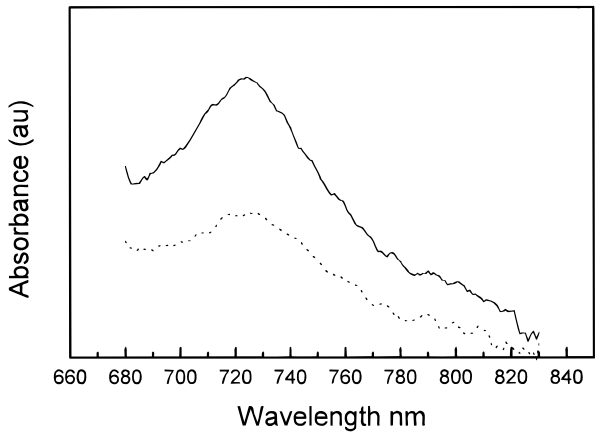

Figure 7. Transient spectra for ZCPINI in toluene for the 680−830 nm spectral region for time delays of (—) 300 fs and (- - -) 1.3 ps. The data illustrate that a charge-separated state is formed within the time resolution of the laser system and that the final charge-separated state is formed in less than 2 ps.

simple considerations of differences in either the static or high-frequency dielectric constants for the four solvents discussed above are at work. This point is discussed in more detail below.

Further analysis of the triad data reveals that, although the appearance of NI^- in Figure 4a is very evident, it is not manifested as an additional exponential rise in the transient absorption data in the triad data shown in Figure 3. This is due to the fact that the yield of the final charge-separated state in *p*-dioxane is less than unity, and the disappearance of ZC^+ due to the return of ZC^+PI^-NI to the ground state offsets the increased absorbance at 470 nm with the appearance of NI^-. This is the reason that the transient absorption data at 470 nm within the triad appear as a decay to the final charge-separated state, whereas charge separation within the dyad appears as a rise in signal due to the nearly unit quantum yield.

In order to obtain the quantum yield of ZC^+PINI^- in *p*-dioxane, we need to obtain the rate constant of the charge shift reaction $ZC^+PI^-NI \rightarrow ZC^+PINI^-$ and the rate constant of charge recombination to ground state from ZC^+PI^-NI. The disappearance of ZC^+PI^-NI within the triad occurs in 26 ± 2 ps, as judged by the transient kinetics at 720 nm. However, this is a sum of the rate constants for charge recombination to

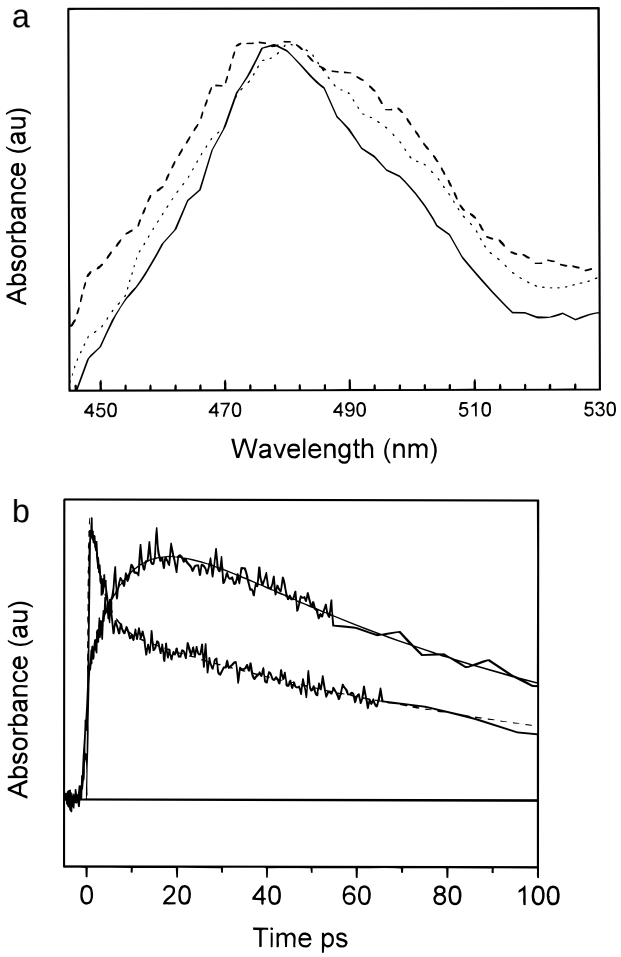

Figure 8. (a) Transient spectra for ZCNI in *p*-dioxane for the 440−530 nm spectral region for time delays of (- - -) 1.5 ps, (•••) 3.5 ps, and (—) 13.5 ps. A time-dependent narrowing of the band is observed, though not as great as for PI^- in the triad. (b) Transient kinetics for ZCNI in *p*-dioxane at 800 nm (dashed fit) and 475 nm (solid fit). The kinetics illustrate the faster decay kinetics for ZC* of 2.9 ps versus the NI^- appearance time of 8.6 ps.

yield ground state and the charge shift reaction to yield ZC^+PINI^-. We were able to determine the back electron transfer rate of ZC^+PI^-NI by obtaining pump−probe data at 810 nm, where PI^- and NI^- do not have appreciable absorptions. A triexponential decay and a long-lived shelf were observed in the data. From this data we obtain a formation time of 1.9 ps for ZC^+, a 44 ps decay time for ZC^+ to ZC due to back electron transfer from ZC^+PI^-NI, and a 2.2 ns decay for the final charge-separated state. The remaining shelf was again most likely due to formation of ^3ZC. Since the charge recombination time of ZC^+PINI^- is long compared to the forward charge separation, we can assume that the rate of decay of PI^- is simply the sum of the rates of charge return to ground state and continued charge separation to NI^-. This gives a value of 59 ps for the formation of ZC^+PINI^- and a quantum yield of 0.4. The formation time is in good agreement with the appearance of the NI^- absorption band at 470 nm in the transient spectra.

We performed similar transient absorption kinetic and spectral measurements on the dyad molecules. Spectra illustrating the time dependence of the 470 nm band of NI^- are illustrated in Figure 8a. A narrowing of the band is observed as the ion pair forms, although not nearly as dramatically as observed for the triad case. The initial broadening of the band is also symmetric, instead of asymmetrically enhanced on the red tail of the absorption as in the triad case. There is also a large difference

in the rate constants for the disappearance of the excited state of the donor and the formation of the reduced acceptor. An example of this is illustrated in Figure 8b for ZCNI in *p*-dioxane. The fast decay at 800 nm is the decay of the excited state of ZC to ZC^+, and the 480 nm signal is due primarily to the appearance of NI^-. The excited state disappears in 2.9 ps and NI^- appears in 8.6 ps. For a simple charge separation process, these two values should be equal. In fact, the decay of the excited state of the donor or acceptor is identified as the charge separation time for many electron transfer reactions. The ramifications of this observation are discussed below. It should be pointed out here that the excited state and cationic state of the donor have an isosbestic point at 470 nm so that only the pulse width limited initial excited state formation and the single exponential rise of the reduced acceptor band are observed.

Discussion

Vibrational Broadening of PI^- within the Triad. The narrowing of the initially asymmetric PI^- absorption band as a function of time can be interpreted as due to vibrational cooling of the reduced species. The tail on the red edge of the absorption band is typical of an intermediate with a vibrationally excited ground state, which possesses lower energy vibronic transitions to its electronically excited states.[19−21] The fast formation time of the ion pair is consistent with the creation of a vibrationally excited anion. It should be noted that a Stokes shift can result when an ion pair or excited state is formed that is not in equilibrium with the solvent.[28−31] This is the result of an increase in the displacement of the electronic manifolds of the ground and excited (or charge transfer) states of a species during the initial steps of solvation. It has been shown to result in a time-dependent red shift of the emission from the charge transfer bands or excited states as solvation ensues. It can also produce a time-dependent blue shift in the absorption bands of these materials. However, we do not believe this is the case here because the initial broadening is asymmetric. Such an increase in the band width of the transition cannot be explained by a Stokes shift but has been readily observed many times in the context of vibrational excitation. Also, the blue edge of the absorption band does not shift as a function of time, further indicating that the primary effect that is observed is an enhancement of the red edge of the band due to vibrational heating.

As outlined above, the observation of vibrational excitation is highly solvent dependent and the relaxation process is primarily due to intermolecular interactions with the solvent. Seilmeier et al. have outlined three mechanisms of intermolecular energy transfer.[19] They are (1) translational collisions, (2) hydrogen bonding interactions, and (3) resonant dipole−dipole interactions. The first mechanism is unlikely because of the similarity of the solvent molecules employed. It seems improbable that *o*-xylene will have a significantly different collisional effect than toluene, for example. It has also been shown that the rate for collisional vibrational relaxation does not vary significantly with the solvent.[20] Hydrogen bonding is ruled out due to the aprotic nature of the solvents and the lack of any acidic protons on ZCPINI. It seems equally unlikely that there is a significant difference in the dipole−dipole interactions of toluene vs *o*-xylene. Given that the intermolecular vibrational relaxation mechanisms should give similar results, other factors must play a role in the observation of vibrational excitation of the triad in *p*-dioxane and *o*-xylene, but not in toluene and benzene.

Table 3. Data for Charge Separation and Recombination for ZCNI in Polar Solvents with Differing Dielectric Relaxation Times

solvent	τ_L (ps)	ϵ_S[37]	τ_{CS} (ps)	τ_{CR} (ps)
butyronitrile	0.5[38]	24.8	0.28	20
pyridine	1.0[39]	12.9	3.7	12
octanenitrile	7.9[38]	13.9	3.7	19

Evidence for Dynamic Solvation of the Triad Ion Pairs. For fast ion pair formation, the well-known dynamic solvent effect may play a role in mediating the rate of electron transfer.[28,29] This effect leads to a breakdown of conventional transition state theory, which assumes that a reaction that proceeds to the transition state will continue to the final state with unity quantum yield. However, dielectric relaxation of the solvent can significantly retard the progress of the transition state in a charge transfer reaction and result in recrossings at the barrier. The time scale for the influence of the solvent is determined by the nature of the motions involved. For example, inertial solvent motions are expected to affect electron transfer rates on a femtosecond time scale, whereas longitudinal relaxation times expected from continuum theory generally modulate the rates on a picosecond time scale.[28]

It is known that the dielectric relaxation times of the solvents utilized in this study occur in the order benzene < toluene < *o*-xylene < *p*-dioxane.[32,33] (These results do not include subpicosecond relaxations.) Although the differences do not scale linearly with the relaxation times, the faster dielectric relaxation of benzene and toluene may explain the faster rate of charge separation in the context of the dynamic solvent effect. Additionally, toluene and benzene have previously been found to have an unusual ability to stabilize ion pairs as evidenced by anomalously fast charge transfer times.[9,34] Other possible mechanisms for the dynamic solvent effect may reflect the involvement of specific solvent vibrational modes in the electron transfer reaction and/or differences in solvent electronic structure. Such electronic structure differences can result in the higher multipole moments of the solvent playing an important role in determining the overall charge distribution in the transition state for the electron transfer reaction.

Solvation of the Dyads. As discussed above, the ZCNI dyad data show spectral broadening of the reduced acceptor and also a difference of almost a factor of 3 in the kinetics of the decay of the excited state of the donor and the rise time of the reduced electron acceptor. The difference in the appearance times of the cation and anion radicals could be due to the formation of a vibrationally hot acceptor and/or solvation effects. However, for this case, we do not believe that the broadening is due to formation of a vibrationally hot acceptor because no evidence for a vibrationally enhanced red edge of the absorption band exists as is characteristic of vibrationally hot species. Rather, the broadening of the band is symmetric around the absorption peak.

In order to further probe these effects, we performed pump probe data on ZCNI in polar solvents, in which the dielectric relaxation times are better characterized relative to the nonpolar solvents discussed above. The results are presented in Table 3. The data are compared to the longitudinal dielectric relaxation time (τ_L) of the solvent, which is related to the Debye

(28) Barbara, P. F.; Walker, G. C.; Smith, T. P. *Science* **1992**, *256*, 975 and references therein.
(29) Barbara, P. F.; Jarzeba, W. *Acc. Chem. Res.* **1988**, *21*, 195 and references therein.
(30) Maroncelli, M.; Fleming, G. R. *J. Chem. Phys.* **1987**, *86*, 6221.
(31) Simon, J. D.; Su, S.-G. *Chem. Phys.* **1991**, *152*, 143.
(32) Srivastava, S. C.; Sinha, M. S. *J. Phys. Soc. Jpn.* **1977**, *43*, 1361.
(33) Petro, A. J.; Smyth, C. P. *J. Am. Chem. Soc.* **1957**, *79*, 6142.
(34) Warman, J. A.; Smit, K. J.; de Haas, M. P.; Jonker, S. A.; Paddon-Row, M. N.; Oliver, A. M.; Kroon, J.; Ouvering, H.; Verhoeven, J. W. *J. Phys. Chem.* **1991**, *95*, 1979.

relaxation time (τ_D) and the static frequency (ϵ_S) and high-frequency (ϵ_O) dielectric constants of the solvent by the relation $\tau_L = (\epsilon_o/\epsilon_s)\tau_D$.[28] In the nitrile solvents, the rates of electron transfer were significantly faster than τ_L, implying that intramolecular vibrational modes must play a larger role than solvent relaxation in charge separation within these molecules.[17,35,36] Theory has been developed for such cases, where high-frequency intramolecular vibrational modes that are coupled to the electron transfer coordinate are considered, in addition to the dielectric relaxation rate of the solvent.[35,36] The rates of electron transfer observed here are also very high even in nonpolar media, in spite of relatively low free energies of reaction. The fact that charge separation occurs faster than the typical relaxation time of the solvents implies that the ion pair is prepared without a fully-formed solvation shell and that broadening of the easily observed anion absorption band is possibly due to the large inhomogeneity of solvation at early times. This possibility is made even more likely because these bandwidths are highly sensitive to the static dielectric constant of the solvents, broadening in more polar media. Thus, the band width of the absorption of NI^- can be thought of as a sensitive probe of solvation.

The data for ZCPI, which has a free energy of charge separation that is about 0.3 eV more positive than that of ZCNI, also lend support for solvation effects upon the absorption band of the reduced acceptor. In *p*-dioxane, the excited state of ZC decays in 15 ps, whereas the ion pair appears in 21 ps. The ratio of these values is much closer to unity than the factor of 3 found for ZCNI, which implies that the solvent molecules are better able to fully solvate the ion pair as it forms.

Conclusions

Results are presented on a triad supramolecular system that undergoes charge separation upon photoexcitation. The ZCPINI molecule possesses acceptors with well-defined and well-separated absorption spectra, permitting unambiguous observation of intermediates in the charge separation reaction. The triad system undergoes electron transfer 1 order of magnitude faster than the control molecule ZCPI and has a charge separated lifetime 50 times longer. Cyclic voltammetry experiments show that the covalently linked PINI acceptors are more easily reduced by 0.1−0.2 V than the individual PI and NI moieties. This plays a significant role in producing faster electron transfer in the triads than within the dyad control molecules. Broadening of the intermediate PI^- acceptor band in ZCPINI is observed and attributed to vibrational relaxation of the chromophore on a 4.5 ps time scale. Large differences in the charge separation rates in similar low-polarity solvents are observed and attributed to dynamic solvent effects. The data are compared to those of the dyad systems, which can display faster charge separation times than the longitudinal dielectric relaxation times of the solvents. This is attributed to high-frequency intramolecular vibrational modes coupled to electron transfer. Time-dependent broadening of the normally sharp absorption bands of the reduced acceptors is found to be a sensitive probe of solvation. These data show that the course of a multistep electron transfer reaction can be exquisitely sensitive to the detailed nature of the surrounding medium and that these sensitivities go far beyond simple considerations of solvent dielectric properties. Molecules such as ZCPINI can be used successfully to probe these intricacies.

Experimental Section

Proton NMR spectra were obtained on a Bruker AM-300 300 MHz spectrometer. Mass spectra were obtained with a Kratos MALDI spectrometer. UV−visible spectra were obtained with a Shimadzu UV-160 spectrometer. Merck silica gel 60 was used for column chromatography. The preparation of ZCPI was reported earlier.[40]

Synthesis. *N*-Octylnaphthalene-1,8-dicarboxyanhydride-4,5-dicarboximide (1). 1,4,5,8-Naphthalenetetracarboxylic acid dianhydride (20.0 g, 0.0746 mol) is refluxed under nitrogen with stirring in DMF (200 mL). A brownish slurry results. 1-Aminooctane (9.64 g, 0.0746 mol) is added dropwise down the condenser over 5 min. The reaction is refluxed for 15 h, then cooled in the refrigerator for 2 h. The white slurry of the bisimide is suction filtered. The oily DMF filtrate is stripped to near dryness on a rotary evaporator and taken up in *p*-xylene, and the solvent is evaporated again to yield 26.0 g of crude monoimide, bisimide, and dianhydride starting material. The oily residue is chromatographed on silica gel with dichloromethane to yield 7.59 g of pure monoimide, 26.8%: mp 180−183 °C; vis in chloroform (nm) 354, 374; MS 380.8 (calcd 379.4); ^{1}H NMR (δ in $CDCl_3$) 8.82 (s, 4 H, naphthalene monoimide rings), 4.20 (t, 2 H, *N*-methylene), 1.28 (broad singlet, 12 H, octyl chain), 0.88 (t, 3 H, 6.6 Hz, octyl chain methyl).

***N*-Amino-*N*′-octylnaphthalene-1,8:4,5-tetracarboxydiimide (2).** Monoimide **1** (758 mg, 2 mmol) and hydrazine (125 mg, 2.6 mmol) are refluxed under nitrogen with stirring in DMF (20 mL) for 2 h. The DMF is stripped on a rotary evaporator, and the residue is chromatographed on silica gel using 5% methanol/chloroform to yield 697 mg of pure **2**, 90%: vis in chloroform (nm) 354, 374; MS 394.0 (calcd 393.4); ^{1}H NMR (δ in $CDCl_3$) 8.78 (d, 4 H, naphthalene ring), 5.58 (s, NH_2), 4.17 (t, 2 H, *N*-methylene), 1.74 (m, 2 H, octyl chain), 1.40 (m, 2 H, octyl chain) 1.28 (broad multiplet, 8 H, octyl chain), 0.88 (t, 3 H, 6.6 Hz, octyl chain methyl).

HC-NI. Methyl 3^2-(*trans*-4-aminophenyl)-13^1-desoxopyropheophorbide *a* (**3**)[40] (20 mg, 0.0319 mmol) and **1** (72.8 mg, 0.192 mmol) are refluxed under nitrogen with stirring in pyridine (5 mL) for 6 h. The reaction mixture is cooled, and the solvent is removed with a rotary evaporator. The residue is chromatographed on silica gel with 3% acetone/chloroform (v/v) to yield 15.1 mg of HC-NI, 47.9%: vis in chloroform (nm) 362 and 381 (bisimide), 420, 508, 540.5, 599, 656.5; MS 987.9 (calcd 987.2); ^{1}H NMR (δ in $CDCl_3$) 9.72, 9.55, 9.40 (singlets, 1 H 10, 5, 20), 8.51, 7.71 (dd, 2 H, 16.4 Hz, trans double bond), 7.96, 7.78 (dd, 4 H, 7.5 Hz, naphthalene bisimide rings), 7.21, 6.53 (very broad singlets, 4 H, *p*-disubstituted benzene ring), 4.96 (m, 2 H, ring E), 4.74 (q, 1 H, 7.3 Hz, ring D), 4.58 (d, 1 H, 9.3 Hz, ring D), 4.14, 3.15 (broad multiplets, 5 H, propionic acid side chain and *N*-methylene), 3.87 (q, 2 H, 7.6 Hz, ring B ethyl), 3.74, 3.72, 3.57, 3.44 (singlets, 3 H each, methyl groups), 2.80 (m, 1 H, propionic acid side chain), 2.59 (m, 2 H, propionic acid side chain), 2.18 (d, 3 H, 7.0 Hz, ring D methyl), 1.98 (t, 3 H, 7.3 Hz, ring B ethyl), 1.20 (broad singlet, 10 H, octyl chain), 0.86 (t, 3 H, 6.2 Hz, octyl chain methyl), −2.72, −4.97 (singlets, 1 H each, NH of phorbin).

ZC-NI. A small amount of HC-NI is dissolved in a mixture of chloroform/methanol 3:1 (v/v) 5 mL). A few crystals of zinc acetate dihydrate are added, and the mixture is refluxed under nitrogen with stirring for 30 min. The reaction mixture is then poured into water, chloroform is added, and the organic layer separated, washed 3× with water, and dried over anhydrous sodium sulfate. There is quantitative conversion to the metallochlorin. Vis in *p*-dioxane (nm): 362.5 and 382.5 (bisimide), 426.5, 520.5, 635. MS: 1050.9 (calcd 1050.6).

HCPINI. Compounds **3** (20.0 mg, 0.0319 mmol), **1** (12.6 mg, 0.0319 mmol), and pyromellitic dianhydride (7.0 mg, 0.032 mmol) are refluxed together with stirring under nitrogen in pyridine (10 mL) for 4.5 h. Analysis of the reaction by prep TLC/mass spectrometry showed that a fast-moving band at $R_f = 0.9$ that eluted with 10% acetone/chloroform (v/v) is the desired product. The pyridine is evaporated in a stream of nitrogen, and the residue preparative TLCed on silica gel with 10% acetone/chloroform (v/v). The fast eluting zone is scraped

(35) Sumi, H.; Marcus, R. A. *J. Chem. Phys.* **1986**, *84*, 4894.
(36) Jortner, J.; Bixon, M. *J. Chem. Phys.* **1988**, *88*, 167.
(37) Riddick, J. A.; Bunger, W. B.; Sakano, T. K. *Organic Solvents*; Wiley and Sons: New York, 1986.
(38) Dutt, G. B.; Doraiswamy, S. In *Ultrafast Processes in Spectroscopy*; IOP: Bayreuth, Germany, 1992; p 531.
(39) van der Zwan, G.; Hynes, J. T. *Chem. Phys. Lett.* **1983**, *101*, 367.
(40) Wiederrecht, G. P.; Svec, W. A.; Niemczyk, M. P.; Wasielewski, M. R. *J. Phys. Chem.* **1995**, *99*, 8918.

off the plate, and the product is leached off the silica gel with acetone to yield HCPINI, 2.5 mg, 6.5%: vis in chloroform (nm) 378.5 (naphthalene bisimide), 428.5, 508, 539, 652.5; MS 1201.4 (calcd 1201.7); ^{1}H NMR (δ in $CDCl_3$) 10.27, 9.36, 8.88 (singlets, 1 H each, 10, 5, 20), 8.77, 7.63 (dd, 2 H, 16.3 Hz, trans double bond), 8.31 (s, 2 H, pyromellitic bisimide ring), 8.15, 7.80 (dd, 4 H, 8.3 Hz, naphthalene bisimide rings), 7.11, 6.38 (broad singlets, 2 H each, *p*-disubstituted benzene ring), 4.94 (m, 2 H, ring E), 4.75 (q, 1 H, 7.0 Hz, ring D), 4.52 (d, 1 H, 9.0 Hz, ring D), 4.12 (m, 2 H, octyl chain), 3.83 (q, 2 H, 7.5 Hz, ring B ethyl), 3.78, 3.75, 3.65, 3.55 (singlets, 3 H each, methyl groups), 3.17, 2.83 (broad multiplets, 1 H each, propionic acid side chain), 2.97 (broad multiplet, 2 H, octyl chain), 2.60 (broad multiplet, 2 H, propionic acid side chain), 2.13 (broad singlet, 3 H, ring D methyl), 1.97 (t, 3 H, 7.5 Hz, ring B ethyl), 1.18 (m, 10 H, octyl chain), 0.85 (t, 3 H, 7.1Hz, octyl chain methyl), −2.81, −5.58 (singlets, 1 H each, NH of phorbin).

ZCPINI. A small amount of HCPINI is metalated in the same manner as HCPI above: vis in *p*-dioxane (nm) 381 (naphthalene bisimide), 423.5, 509, 543.5, 583.5, 634.5; MS 1264.3 (calcd 1264.7).

Electrochemistry. Cyclic voltammetry was used to determine the redox potentials of the molecules. A model 273 EG&G Princeton Applied Research potentiostat was used in conjunction with a silver/silver ion reference electrode (BAS) for the nonaqueous measurements. Redox potentials were internally referenced to ferrocene, for which $E_{1/2}$ for oxidation in benzonitrile is 0.40 V vs SCE. The measurements were performed in benzonitrile (HPLC grade)/0.1 M tetra-*n*-butylammonium perchlorate using a platinum disc electrode.

Spectroscopy. Transient absorption data were obtained in *p*-dioxane, toluene, benzene, and *o*-xylene. *p*-Dioxane was freshly distilled from lithium aluminum hydride prior to use, while toluene, benzene, and *o*-xylene (HPLC grade) were dried over 3A molecular sieves.

The experimental system consists of a homemade CW mode-locked YAG laser based on a Quantronix 416E head that is frequency doubled with a 15 mm noncritically phase matched LBO crystal to produce 3 W of 532 nm light at an 82 MHz repetition rate. The output is used to synchronously pump a linear dye laser with a saturable absorber and a prism pair for short pulse generation. Rhodamine B was used as the gain medium and oxazine 720 as the saturable absorber. This dye combination produces a 200 mW pulse train at 640 nm with a 250 fs duration. The dye pulses are frequency chirped in a 35 cm length of single-mode, polarization-preserving optical fiber, then amplified at a 1 kHz repetition rate by a three-stage DCM dye amplifier pumped by the frequency-doubled output (532 nm, 700 mW) of a homemade Nd:YAG regenerative amplifier.[41] The amplified pulses were recompressed using two passes through a pair of SF-14 prisms to yield 25 μJ, 100 fs, 640 nm pulses. Fifty percent of the output is used to generate a white-light continuum by focusing it with a 15 cm focal length lens into a 0.5 cm thick block of fused silica. Careful adjustments of the intensity and position of the quartz relative to the beam waist results in shot-to-shot fluctuations in the white light of less than 5%. The block is rotated at 12 rpm to prevent damage. A pair of 300 grooves/mm gratings spaced approximately 2 cm apart are used to compensate for group velocity dispersion in the quartz, resulting in an instrumental time response of approximately 130 fs.

The energy of the red excitation light on the sample was varied using a polarizer−λ/2 wave plate combination. Typically, 2−5 μJ was used to excite the molecules. The excitation beam was chopped at 500 Hz synchronized to the laser repetition rate. The white-light probe beam was split into measuring and reference beams. The arrival of the measuring probe beam relative to the excitation beam was accomplished with an optical delay line that used a linear stepping motor (Compumotor) with 1 μm resolution. The nearly collinear and codirectional excitation and measuring probe beams were focused into the sample to a 0.3 mm diameter. The sample was contained in a 1 cm pathlength cuvette and was stirred. The wavelength of the measuring and reference probe beams were selected with a SPEX M270 monochromator. Changes in the transmission of the measuring probe light through the sample and changes in the reference probe beam were monitored by photodiodes. The output of each photodiode was integrated by a gated integrator (Evans), and both signals were digitized and recorded by a personal computer (Gateway 66 MHz, 486). The data acquisition software monitored the quality of each shot and only averaged shots within 10% of the average intensity of the reference probe beam level. Kinetic parameters were obtained by iterative reconvolution using the Levenberg−Marquardt algorithm. Transient absorption spectra at a particular time were obtained by allowing the computer to repetitively scan the monochromator at a fixed delay time between the pump and measuring probe beams. Typically, 20 wavelength scans were averaged.

Acknowledgment. The authors wish to acknowledge the support of the Division of Chemical Sciences, Office of Basic Energy Sciences, U.S. Department of Energy, under Contract W-31-109-Eng-38. The authors also wish to thank Paul Barbara, Marshall Newton, and Ken Spears for insightful discussions.

JA953159Y

(41) Postlewaite, J. C.; Miers, J. B.; Reiner, C. C.; Dlott, D. D. *IEEE J. Quant. Elec.* **1988**, *24*, 411.